

ARTICLE

Eu@COK-16, a host sensitized, hybrid luminescent metal-organic framework

Cite this: DOI: 10.1039/x0xx00000x

D. Mustafa,^{a,b,*} I. G. N. Silva,^a S. R. Bajpe^{b,†} J. A. Martens,^b C. E. A. Kirschhock^b, E. Breynaert^{b,*} and H. F. Brito^a

Received 00th January 2012,
Accepted 00th January 2012

DOI: 10.1039/x0xx00000x

www.rsc.org/

A new concept of luminescent host-guest materials was developed by introduction of Eu^{3+} into COK-16, a HKUST-1 type hybrid metal-organic framework (MOF) with cation exchange properties. In Eu@COK-16, the luminescent ion resides in the pore system of the MOF. The luminescent properties of Eu@COK-16 have been studied based on excitation and emission, allowing analysis of intramolecular energy-transfer processes from the COK-16 host to the exchanged Eu^{3+} ions. Both, the framework trimesate (BTC) and encapsulated $[\text{PW}_{12}\text{O}_{40}]^{3-}$ ions contribute to energy transfer. Since the *antenna* molecules (BTC) are part of the framework structure and $[\text{PW}_{12}\text{O}_{40}]^{3-}$ ions only partly occupy one of the three types of cavities in the structure, a large fraction of the pore volume in this host sensitized luminescent MOF remains available for catalysis applications or adsorption of additional sensitizing molecules. The material structure was determined from a combination of elemental analysis, XAS, XRD, electron and luminescence spectroscopy.

Introduction

Trivalent rare earth ions (RE^{3+}) exchanged in zeolites, grafted onto the walls of mesoporous (semi)-metal oxides or being nodes in metal organic frameworks (MOFs) have attracted attention both as luminescent material and as catalyst.^{1–4} Key aspect for this interest is the presence of luminescent centers in a well-defined pore system offering the ability to accommodate guest molecules close to the luminescent species.⁵ In case of zeolites and mesoporous silicates, the RE^{3+} ions and the sensitizing molecules reside in the pores of the materials. With the discovery of RE^{3+} based MOFs, the luminescent ions and the sensitizing ligands no longer occupy the cavities but are part of the framework structure itself.⁶ The rigid organization of the linkers in the MOF structure not only induces increased luminescence lifetimes,⁷ but also results in additional free pore space for adsorption of additional sensitizing molecules or reactants. Disadvantage of embedding of the RE^{3+} ions into the framework is their higher coordination number, leaving less options for tailoring their photo luminescent or catalytic properties.

The synthesis of Eu@COK-16, demonstrates an intermediate approach where the sensitizing ligands are part of a porous MOF framework, while the RE^{3+} ions are introduced into the pores via ion exchange, similar to the situation occurring in zeolites. The synthesis of the COK-16⁸ structure uses Keggin type $[\text{PW}_{12}\text{O}_{40}]^{3-}$ polyoxometalate anions as template.^{9,10} The $[\text{PW}_{12}\text{O}_{40}]^{3-}$ ions retain their negative charges upon inclusion in the COK-16 structure, hence

providing cation exchange properties to the otherwise neutral $\text{Cu}_3(\text{BTC})_2 \cdot 3\text{H}_2\text{O}$ framework.⁸ In addition, the POM inclusion also dramatically improves the material stability in steam conditions as compared to the HKUST-1 MOF with the same framework topology and composition.¹¹

Results and discussion

In the as-synthesized COK-16 the negative charge of the encapsulated polyoxometalate is compensated by extra-framework Cu^{2+} ions. Using a highly Cu^{2+} selective di-iminoacetate resin, these extra Cu^{2+} ions can selectively be exchanged for Na^+ while the MOF structure remains intact.⁸ The high affinity of polyoxometalate anions for trivalent rare earth ions^{12,13} allows exchanging COK-16 directly with the RE^{3+} ions. In case of europium, this yields the Eu^{3+} exchanged COK-16 as the first example of a new class of hybrid luminescent materials, where the luminescent ions reside in the pore system of a framework which acts as an *antenna*. This leaves the RE^{3+} ions more available for interaction with other ions and/or ligands. Eu^{3+} was chosen because of its characteristic narrow emission bands originating from 4f intra-configurational transition that can be used as a luminescent probe for the local environment of this ion.¹⁴ Vacuum dried COK-16 crystals were suspended in a 50% vol. ethanol-water solution containing EuCl_3 with a $\text{Eu}^{3+}:[\text{PW}_{12}\text{O}_{40}]^{3-}$ ratio of respectively 1 and 10. Upon increasing exchange of COK-16 with Eu^{3+} , as indicated by the increasing emission intensity of the

hypersensitive transition $^5D_0 \rightarrow ^7F_2$ (618 nm) of Eu^{3+} , Cu^{2+} ions are released into solution (see Figure S1 and Figure S2). After equilibration (up to 10 days), the crystals were washed twice with absolute ethanol to remove superfluous Eu^{3+} , before drying under reduced pressure at room temperature.

The higher stability constants documented for RE^{3+} as compared to Cu^{2+} complexes with the mellitic acid series^{15,16} indicated a risk for COK-16 breakdown and conversion into $\text{Eu}(\text{BTC}) \cdot 6\text{H}_2\text{O}$ structures. Therefore, the integrity of the COK-16 framework during Eu^{3+} exchange was monitored with a combination of bulk and local techniques such as Powder X-Ray Diffraction (PXRD), Extended X-ray Absorption Fine Structure (EXAFS) and Scanning Electron Microscopy (SEM).

Evaluation of the PXRD patterns of the Eu^{3+} exchanged COK-16 samples (see Figure S3) revealed a fully intact COK-16 framework structure for all samples except those contacted with a 10:1 $\text{Eu}^{3+}:[\text{PW}_{12}\text{O}_{40}]^{3-}$ ratio for 7 days. In these last samples a minute fraction of $\text{Eu}(\text{BTC}) \cdot 6\text{H}_2\text{O}$ is formed as result of framework degradation due to competition between Cu^{2+} and Eu^{3+} for the framework linkers. This result was corroborated by the SEM analysis (Figure 1) confirming the absence of morphological changes of the COK-16 MOFs for samples exchanged with Eu (1 Eu^{3+} : 1 $[\text{PW}_{12}\text{O}_{40}]^{3-}$ dosed) and revealing the appearance of a minute fraction of needle-like $\text{Eu}(\text{BTC}) \cdot 6\text{H}_2\text{O}$ crystals in 10:1 samples equilibrated for 7 days, respectively (see Figure S4). SEM-EDX mappings demonstrate a uniform distribution of Cu and Eu over the crystals, as would be expected for Eu^{3+} exchanged COK-16 (see Figure S5).

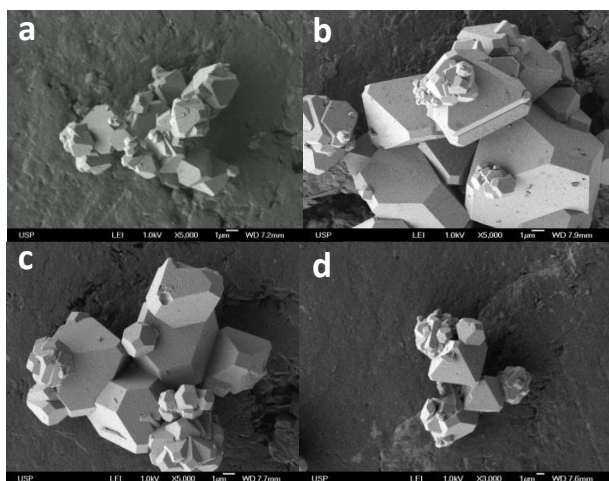


Figure 1: Scanning Electron Microscopy of the COK-16. a) as prepared. b), c) and d) COK-16 with 1 Eu^{3+} : 1 $[\text{PW}_{12}\text{O}_{40}]^{3-}$ exchanged for 1, 2 and 7 days respectively.

The local chemical environment of Eu and its position in the COK-16 sample was elucidated by combining X-ray Absorption Spectroscopy (Figure 2, Table 1) with Rietveld refinement of the PXRD patterns (Figure 3). As shown in Figure 2, EXAFS single scattering analysis revealed the Eu^{3+} ion occurs in a non-centrosymmetric 9-coordinated site near the surface of the $[\text{PW}_{12}\text{O}_{40}]^{3-}$ ions responsible for the cation exchange properties of COK-16. This information served to localize the exchange Eu^{3+} inside the structure of COK-16 by Rietveld refinement. Only one Eu position was consistent with identical distances of 3.7 Å between the rare earth and four tungsten ions of the Keggin ion, which showed an occupation factor of roughly 75% of the available cavities of type L2 in the HKUST-1 topology.^{8,17} The occupation of the Eu^{3+} freely converged to 1 Eu^{3+} ion per Keggin ion. In addition to the 4 O atoms from $[\text{PW}_{12}\text{O}_{40}]^{3-}$ at a distance of 2.5 Å,

the coordination of Eu is completed with 4 water molecules at a distance of 2.3 Å, identified by inspection of the observed electron density map. This map also showed considerable electron density in the L3 cavity of the MOF which is unoccupied by Keggin ions. This electron density was assigned to BTC molecule, occluded by selective adsorption from the initial synthesis mixture.^{18,19} For the refinement it was treated as freely reorienting rigid body. In the resulting $\text{Eu}@\text{COK-16}$, this molecule assumed a position where one of its carboxylate groups is in interaction distance to europium (Eu-O 2.4 Å) (Figure 3). Interestingly, the occluded BTC molecule also is in direct interaction with the framework via a copper pair of the occluding cavity (Cu-O 2.2 Å). This coordination of Eu^{3+} results in a square anti-prisma consisting of oxygen from Keggin and water, which is capped on one square face by an oxygen from the extra framework BTC molecule (Figure 4). The local symmetry of this coordination is consistent with C_{4v} symmetry in the first coordination sphere of europium. This local geometry is confirmed by the luminescence spectra obtained at 77 and 298 K.

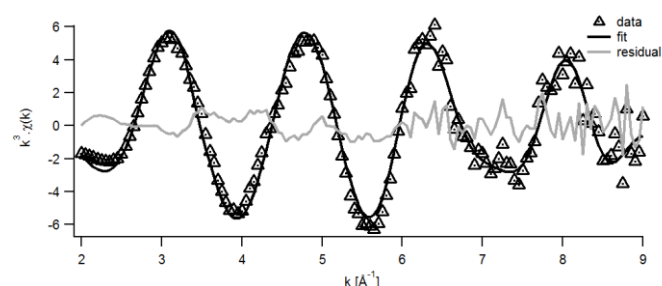


Figure 2: k^3 -weighted EXAFS data, fit and residual for sample 1Eu7d.

Table 1: Geometric parameters obtained by shell fitting k^2 and k^3 -weighted data for the EXAFS spectrum in Figure 2.

Atom	Number	DW-factor	Distance
O	4	0.00200 ^s	2.35
O	5	0.00397	2.48
W	4	0.00813	3.69

$E^0 = 9.715$; $S_0^2 = 1$.

^snot floated during fit

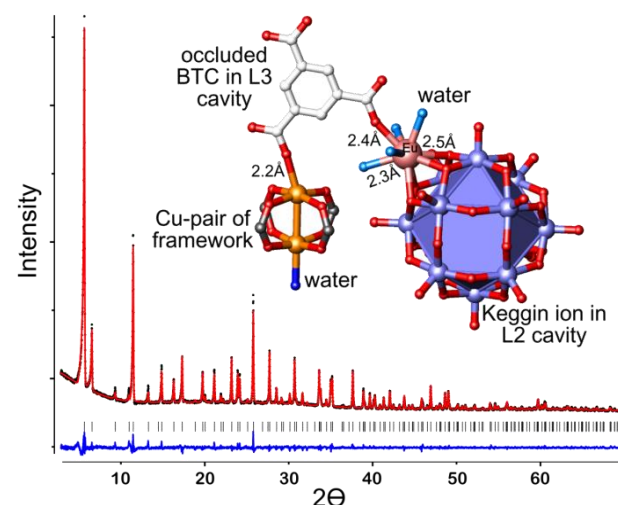


Figure 3: Rietveld refined powder pattern of sample 1Eu-7d (-factor 4.7%, weighted R-factor 8.5, RF^2 -factor 12%). The local geometry of Eu^{3+} is shown as inset.

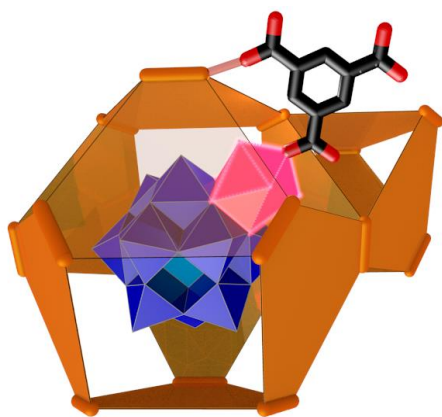


Figure 4: Global arrangement of Eu in COK-16 determined by modeling the XAS spectra in combination with Rietveld refinement of the PXRD patterns.

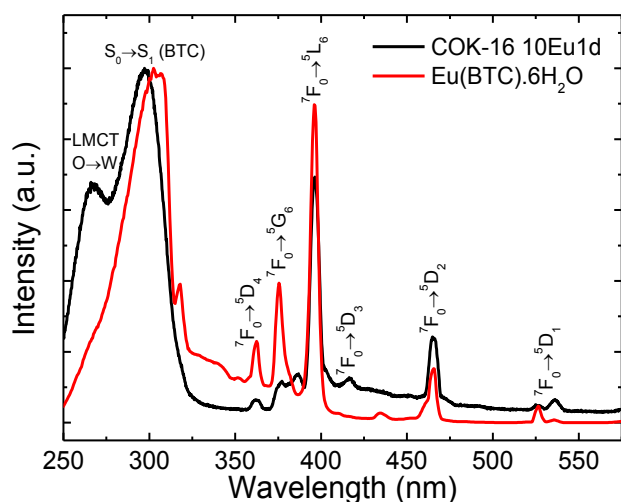


Figure 5: Excitation spectra for the Eu(BTC).6H₂O and COK-16 with Eu³⁺ (10 Eu³⁺: 1 [PW₁₂O₄₀]³⁻) monitoring the hypersensitive ⁵D₀→⁷F₂ transition at 618 nm recorded at 77 K.

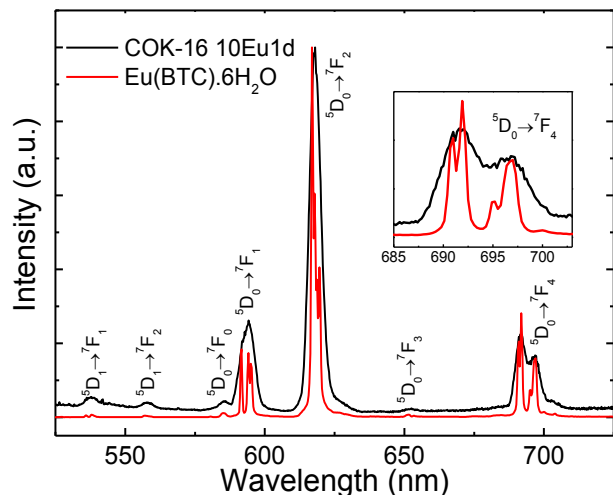


Figure 6: Emission spectra for the Eu(BTC).6H₂O and COK-16 with Eu³⁺ (10 Eu³⁺: 1 [PW₁₂O₄₀]³⁻) excited at 295 nm recorded at 77 K.

Comparison of the excitation spectra of the Eu(BTC).6H₂O and Eu@COK-16 recorded at 77 K (Figure 5) indicates the presence of a new broad absorption band around 265 nm which is assigned to a ligand-to-metal charge-transfer O→W, LMCT transition.^{20,21} This transition is overlapped by an intense absorption band at 295 nm assigned to the S₀→S₁ transition of BTC. In addition, narrow absorption bands between 350 and 550 nm assigned to the ⁷F₀→⁵L_J intra-configurational transitions of the Eu³⁺ ion are observed.²² The absorption bands observed in the Eu@COK-16 excitation spectrum confirm the close association of Eu³⁺ with the [PW₁₂O₄₀]³⁻ ions residing in the pores of COK-16 and the sensitizing role of BTC. In addition, the appearance of the O→W LMCT band and shift of the BTC ligand band to higher energies readily indicate a different chemical environment for Eu³⁺ in Eu@COK-16 as compared to Eu(BTC).6H₂O.

The emission spectra (Figure 6) present the narrow bands that can be assigned to the ⁵D₀→⁷F_J transitions (J = 0, 1, 2, 3, 4) of the Eu³⁺ under excitation in the BTC absorption band at 295 nm. The presence of a ⁵D₀→⁷F₂ band of highest intensity indicates that the Eu³⁺ ion is found in chemical environment without inversion centre hence corroborating the structural analysis. In such a case, the Laporte's rule is slightly relaxed for 4f–4f transitions due to mixing of opposite parity electronic configurations, resulting from odd components of non-centro-symmetric ligand fields.²³ The broadening of the 4f–4f transitions of the Eu³⁺ ion indicates the occurrence of Eu³⁺ in a chemical environment with site symmetry of the type C_s, C_n or C_{nv}, as expected from the local geometry found by EXAFS and Rietveld refinement.

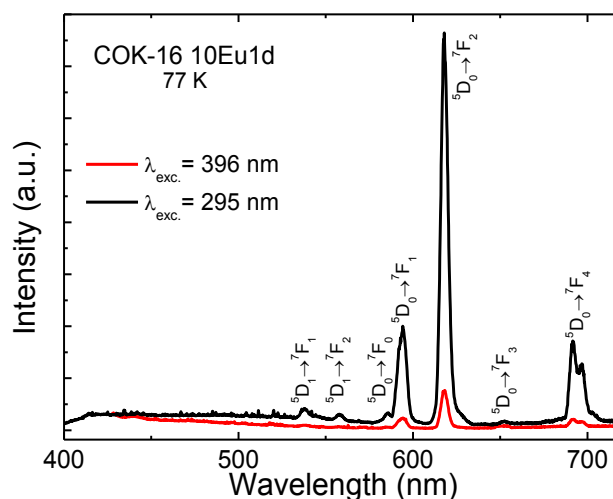


Figure 7: Emission spectra using respectively a 295 and 396 nm excitation wavelength for the Eu@COK-16 sample exchanged for 1d with (10 Eu³⁺: 1 [PW₁₂O₄₀]³⁻).

In the emission spectra for the Eu@COK-16 samples, the broad band resulting from BTC luminescence (between 400 and 500 nm)²⁴ can only be observed in the spectrum of the samples with the lowest concentration of Eu³⁺ (1 Eu³⁺: 1 [PW₁₂O₄₀]³⁻ 1 day, λ_{exc.} = 295 nm) (see Figure S2). Disappearance of this band with

increasing Eu content indicates efficient energy transfer from BTC to the Eu^{3+} ion. This result is corroborated by the higher emission intensity of the $^5\text{D}_0 \rightarrow ^7\text{F}_j$ transitions of Eu^{3+} under excitation in the BTC band (295 nm) as compared to the direct excitation of the Eu^{3+} ion at 396 nm (Figure 7). On the other hand, the moderate emission intensity of the COK-16 is associated with the non-radiative decay channel due to vibronic coupling with the vibrations of the four water molecules in first coordination sphere.²⁵

As a conceptual illustration of potential future developments, excitation and emission spectra were recorded for a Eu@COK16 (1Eu7d) sample, impregnated with DMSO and consequently dried at 393 K to exchange the coordinated water molecules with DMSO (Figure S6 and S7). The observed change in the relative intensities of the $^5\text{D}_0 \rightarrow ^7\text{F}_3$ and $^5\text{D}_0 \rightarrow ^7\text{F}_4$ transitions clearly indicate a modification in the local symmetry of Eu^{3+} which, assuming the absence of structural changes to the framework, would be consistent with the exchange of water ligands with DMSO.

Conclusions

Eu@COK-16 hybrid luminescent MOF was obtained by replacing 'extra-framework' Cu^{2+} ions in COK-16 with Eu^{3+} . Structural characterisation via EXAFS, XRD and luminescence spectroscopy reveals the location of Eu^{3+} in a C_{4v} symmetry next to the encapsulated $[\text{PW}_{12}\text{O}_{40}]^{3-}$ ions which provide the exchange capacity to COK-16. The close association between Eu and the $[\text{PW}_{12}\text{O}_{40}]^{3-}$ ions in the pore system of the trimesic acid based metal organic framework is confirmed by the excitation and emission luminescence spectra demonstrating the energy transfer from both the POM and the BTC ligands to Eu^{3+} . Since the antenna molecules are part of the framework structures and $[\text{PW}_{12}\text{O}_{40}]^{3-}$ ions partly occupy one of the three types of pores in the structure, and a large fraction of the pore volume in this host sensitized luminescent MOF remains available for catalysis applications or adsorption of additional sensitizing molecules.

Experimental

The exchange of COK-16 with Eu^{3+} was evaluated both as function of Eu^{3+} concentration and equilibration time, using as-synthesized, Cu^{2+} exchanged COK-16 samples, prepared as described previously.⁸ After synthesis, the solids were collected, washed twice with absolute ethanol and vacuum dried at room temperature to remove physisorbed solvents.

XAS measurements were performed at the D04BXAFS1 and D08B-XAFS2 beamlines of the Brazilian Synchrotron Light Laboratory (LNLS) – Campinas, Brazil. The Eu L_{III} results were recorded in fluorescence using a 15 element Ge detector. Data processing and analysis was performed using IFEFFIT²⁶ in combination with the open source programming interface Demeter.²⁶ Theoretical phase shifts and amplitudes were calculated using FEFF6²⁷ for the structural model shown in Figure 4.

PXRD patterns were obtained for all samples from 3 to 90° 2 θ using a Stadi P ($\text{CuK}_{\alpha 1}$, STOE & Cie GmbH) in θ –2 θ geometry and capillary mode.

Rietveld refinement was performed using the GSAS software suite on the samples 1 Eu^{3+} : 1 $[\text{PW}_{12}\text{O}_{40}]^{3-}$ for 7d and 10 Eu^{3+} : 1 $[\text{PW}_{12}\text{O}_{40}]^{3-}$ for 3d. Both could be refined with the same structure and occupation factors. As starting model served the known structure of COK-16 and the position of the Eu^{3+} ion, as deduced from XAS. BTC molecules were introduced as rigid bodies and left freely to refine in position and orientation.^{28,29}

The photoluminescence study was based on the excitation and emission spectra recorded at room temperature (300 K) and in liquid nitrogen (77 K). Luminescence spectra were collected both at 298 and at 77 K in front face mode (22.5°) in SPEX-Fluorolog 2 instrument with double monochromators, coupled with a 450 W xenon lamp serving as excitation source.

Acknowledgements

This work was supported by the Flemish Government via long-term structural funding (Methusalem) and an FWO-CNPq collaboration project. D.M., I.G.N.S. and H.F.B. acknowledge financial support from the Fundação de Amparo à Pesquisa do Estado de São Paulo (FAPESP, Brazil), Conselho Nacional de Desenvolvimento Científico e Tecnológico by Brazil-Belgium Bilateral Project (CNPq-FWO), Instituto Nacional de Ciência e Tecnologia de Nanotecnologia para Marcadores Integrados (inct-INAMI, Brazil) and technical support from Laboratório Nacional de Luz Síncrotron (LNLS, Brazil). E.B. acknowledges a fellowship as Postdoctoraal onderzoeker van FWO-Vlaanderen. S. B. acknowledges the European Commission for a current Marie Curie (IEF) FP7 international fellowship.[‡] D.M. and E.B. thank Dr. Mathias Jobbagy for fruitful discussions.

Notes and references

^a Departamento de Química Fundamental, Instituto de Química da Universidade de São Paulo, 05508-900, São Paulo, SP, Brazil. E-mail: dmustafa@iq.usp.br

^b KULeuven, Center for Surface Chemistry and Catalysis, Department of Microbial and Molecular Systems, Kasteelpark Arenberg 23 – box 2461, B-3001 Leuven, Belgium. E-mail: eric.breynaert@biw.kuleuven.be

[‡] Current address: Department of Materials Science and Metallurgy, University of Cambridge, 27 Charles Babbage Road, Cambridge CB3 0FS, UK

[†] hemimellitic, trimellitic, trimesic, pyromellitic and mellitic acid

* $[\text{Eu}(\text{H}_2\text{O})_4(\text{H}_3\text{BTC})\text{PW}_{12}\text{O}_{40}@\text{Cu}_3\text{BTC}_2]$

Electronic Supplementary Information (ESI) available: ICP-AES analyses, emission spectra as function of the equilibration time, Powder XRD Diffraction Patterns, SEM image of the needle-like structure and EDX mapping of Cu and Eu distribution. See DOI: 10.1039/b000000x/

1. K. Binnemans, *Chem. Rev.*, 2009, **109**, 4283–4374.
2. G. J. McManus, J. J. Perry, M. Perry, B. D. Wagner, and M. J. Zaworotko, *J. Am. Chem. Soc.*, 2007, **129**, 9094–9101.
3. M. D. Allendorf, C. A. Bauer, R. K. Bhakta, and R. J. T. Houk, *Chem. Soc. Rev.*, 2009, **38**, 1330–1352.

4. F. Luo and S. R. Batten, *Dalton Trans.*, 2010, **39**, 4485–4488.
5. M. J. Zaworotko, *Nature*, 2008, **451**, 410–411.
6. J. Rocha, L. D. Carlos, F. A. Almeida Paz, and D. Ananias, *Chem. Soc. Rev.*, 2011, **40**, 926–940.
7. B. Chen, Y. Yang, F. Zapata, G. Lin, G. Qian, and E. B. E. B. Lobkovsky, *Adv. Mater.*, 2007, **19**, 1693–1696.
8. S. R. Bajpe, E. Breynaert, A. Martin-Calvo, D. Mustafa, S. Calero, C. E. A. Kirschhock, and J. A. Martens, *Chempluschem*, 2013, **78**, 402–406.
9. S. R. Bajpe, E. Breynaert, D. Mustafa, M. Jobbágy, A. Maes, J. A. Martens, and C. E. A. Kirschhock, *J. Mater. Chem.*, 2011, **21**, 9768–9771.
10. S. R. Bajpe, C. E. A. Kirschhock, A. Aerts, E. Breynaert, G. Absillis, T. N. Parac-Vogt, L. Giebeler, and J. A. Martens, *Chem. – A Eur. J.*, 2010, **16**, 3926–3932.
11. D. Mustafa, E. Breynaert, S. R. Bajpe, J. A. Martens, and C. E. A. Kirschhock, *Chem. Commun.*, 2011, **3**, 8037–8039.
12. C. E. VanPelt, W. J. Crooks, and G. R. Choppin, *Inorganica Chim. Acta*, 2003, **346**, 215–222.
13. C. E. VanPelt, W. J. Crooks, and G. R. Choppin, *Inorganica Chim. Acta*, 2002, **340**, 1–7.
14. O. L. Malta, H. F. Brito, J. F. S. Menezes, F. R. Gonçalves e Silva, S. Alves, F. S. Farias, and A. V. M. de Andrade, *J. Lumin.*, 1997, **75**, 255–268.
15. D. E. Giammar and D. A. Dzombak, *J. Solution Chem.*, 1998, **27**, 89–105.
16. Z.-M. Wang, L. J. van de Burgt, and G. R. Choppin, *Inorganica Chim. Acta*, 1999, **293**, 167–177.
17. J. Getzschmann, I. Senkovska, D. Wallacher, M. Tovar, D. Fairen-Jimenez, T. Düren, J. M. van Baten, R. Krishna, and S. Kaskel, *Microporous Mesoporous Mater.*, 2010, **136**, 50–58.
18. M. Hartmann, S. Kunz, D. Himsl, O. Tangermann, S. Ernst, and A. Wagener, *Langmuir*, 2008, **24**, 8634–42.
19. P. Chowdhury, C. Bikkina, D. Meister, F. Dreisbach, and S. Gumma, *Microporous Mesoporous Mater.*, 2009, **117**, 406–413.
20. W. Bu, L. Wu, X. Zhang, and A. Tang, *J. Phys. Chem. B*, 2003, **107**, 13425–13431.
21. C. A. Kodaira, H. F. Brito, O. L. Malta, and O. A. Serra, *J. Lumin.*, 2003, **101**, 11–21.
22. O. L. Malta, *J. Lumin.*, 1997, **71**, 229–236.
23. P. A. Tanner, *Chem. Soc. Rev.*, 2013, **42**, 5090–5101.
24. X. Zhang, Y.-Y. Huang, Q.-P. Lin, J. Zhang, and Y.-G. Yao, *Dalt. Trans.*, 2013, **42**, 2294–2301.
25. H. F. Brito, O. M. L. Malta, M. C. F. C. Felinto, and E. E. de S. Teotonio, in *The chemistry of metal enolates*, ed. J. Zabicky, John Wiley, 2009, pp. 131–184.
26. B. Ravel and M. Newville, *J. Synchrotron Radiat.*, 2005, **12**, 537–541.
27. S. Zabinsky, J. Rehr, a Ankudinov, R. Albers, and M. Eller, *Phys. Rev. B. Condens. Matter*, 1995, **52**, 2995–3009.
28. B. H. Toby, *J. Appl. Crystallogr.*, 2001, **34**, 210–213.
29. A. Larson and R. Von Dreele, *General Structure Analysis System (GSAS) - Report LAUR 86-748*, Los Alamos, NM, 2004, vol. 748.